

# Diagnostic Tool for Non-Small Cell Lung Cancer (NSCLC) Lyophilized Serum <sup>†</sup>

Mohammed S. Mohammed <sup>1,\*</sup> and Asmaa M. S. Mohammed <sup>2,3</sup><sup>1</sup> Department of Cancer Biology, National Cancer Institute, Cairo University, Cairo 11796, Egypt<sup>2</sup> Department of Biophysics, Faculty of Science, Cairo University, Giza 12613, Egypt; asmaa.famy@hotmail.com<sup>3</sup> Unit of Medical Physics, Department of Radiotherapy, National Cancer Institute, Cairo University, Cairo 11796, Egypt

\* Correspondence: mohammed.sayed@nci.cu.edu.eg or m\_famy@hotmail.com; Tel.: +20-01152226634

<sup>†</sup> Presented at the 2nd International Electronic Conference on Biomedicines, 1–31 March 2023; Available online: <https://ecb2023.sciforum.net/>.

**Abstract:** Background and Objectives: The international protocol used to diagnose non-small cell lung cancer (NSCLC) usually faces an inappropriate result due to the poor diagnostic ability in the early stages. Carcinoembryonic Antigen (CEA), an established serum tumor marker that is used for NSCLC diagnosis, has limited sensitivity and specificity, but, still, it is the predominant complementary detecting tool wherein its results confirm diagnostic radiology findings (PET-CT). Unfortunately, the limited range of its sensitivity is unable to classify approximately one third of patients suffering from NSCLC. Due to a huge number of patients lately classified as NSCLC, the efficacy of the offered treatment is limited. Hence, the importance of discovering, improving, and establishing a new technique that participates in the NSCLC diagnosis is indeed urgent. Methods: The low angle x-ray scattering (LAXS) technique was applied on the lyophilized serum of NSCLC patients to create patient profiles that were able to distinguish the molecular differences between NSCLC patients, avoiding the undesirable radiation exposure to the patients. Results: The created LAXS profile was characterized by two peaks. The first scattering peak at 4.8° was sensitive to molecular alterations in protein structures that were the main characteristic differences from the normal serum. Comparing the measurements of LAXS profiles of NSCLC with the normal sera, the unique first scattering peak at 4.8° was elucidated as a characterization shape and profile for NSCLC and normal individuals. Conclusions: Using the LAXS technique gives us full details at a molecular level that are introduced as a promising tool that could be a supporter in NSCLC early detection.

**Keywords:** non-small cell lung cancer (NSCLC); low-angle X-ray scattering (LAXS) technique; lyophilized serum



**Citation:** Mohammed, M.S.; Mohammed, A.M.S. Diagnostic Tool for Non-Small Cell Lung Cancer (NSCLC) Lyophilized Serum. *Med. Sci. Forum* **2023**, *21*, 47. <https://doi.org/10.3390/ECB2023-14293>

Academic Editor: Zoran Minic

Published: 29 March 2023



**Copyright:** © 2023 by the authors. Licensee MDPI, Basel, Switzerland. This article is an open access article distributed under the terms and conditions of the Creative Commons Attribution (CC BY) license (<https://creativecommons.org/licenses/by/4.0/>).

## 1. Introduction

Cancer is classified as the second disease that causes mortality after cardiovascular disease wherever in developing or developed countries [1]. Lung cancer is leading in mortality among cancer patients in the United States [1], China [2], and globally. It is divided into two main subtypes according to its histologic classification: small cell lung cancer (SCLC)'s ratio is 15–20% [2], whereas non-small cell lung cancer (NSCLC) is distributed among lung cancer patients by ≈80–85% worldwide [1]. According to the National Comprehensive Cancer Network (NCCN)'s 2017 clinical guidelines, less than one fifth of lung cancer patients (17.7%) are alive over five years after diagnosis [1].

NSCLC patients usually develop in the late stage before being diagnosed; their initial diagnoses are based on clinical signs and bio-sample laboratory investigations. Diagnoses are confirmed with molecular diagnostic imaging (i.e., PET-CT, fMRI) [2,3].

In comparison, the importance of histologic examination and its classification is arising from its appropriate sensitivity to the treatment regimen [2].

Patients suffering from this type of cancer are mainly diagnosed by tumor markers, either through histologic biopsy or serologic markers, and are confirmed with radiologic investigations (PET-CT) [4]. The group at a higher risk for lung cancer includes smokers. Routine CT screening enhances the surveillance rate of 20% of the high-risk group [3]. The main obstacle to doing CT screening for each patient is the undesirable radiation exposure hazard, whereas the histologic biopsy is difficult to manipulate more than one time [4]. Several biomarkers have emerged as predictive and prognostic markers for NSCLC. The biomarkers involved in NSCLC prediction include the fusion of ALK with oncogene (e.g., echinoderm microtubule-associated protein-like 4), rearrangements of ROS1 gene, and inductive sensitization of EGFR mutations [5,6]. The NSCLC patients suffering from sensitizing EGFR mutations predominantly will be chemo-resistant to the following therapeutics agents: erlotinib, gefitinib, or afatinib in about nine to thirteen months of EGFR TKI therapy [1].

Two decades ago, the low-angle x-ray scattering (LAXS) technique was previously shown as an applicable promising biophysical tool that has clinical sensitivity towards the structural alterations in lyophilized human serum [7]. Moreover, a scattering peak, which is produced in this technique, elucidated more specific information to the induced molecular alterations in the structural serum protein levels [7–9]. Moreover, previous studies elucidated the sensitivity of the LAXS technique to monitor any changing at the molecular level structure in biological samples [7] to distinguish characteristic profiles for normal and neoplastic breast tissues and the improvement of enhanced imaging techniques [9]. Moreover, it was used in the discriminate criteria of tissues [10].

Clinically, three tumor markers, carcinoembryonic antigen (CEA), cytokeratin 19 fragments antigen (CYFRA21-1), and squamous cell carcinoma antigen (SCCAg), are approved to diagnostic process of NSCLC with the combination of the histopathologic examinations and radiologic investigations PET-CT [10]. In spite of histopathology, the golden marker for NSCLC diagnosis, the manipulation of patient specimen biopsy or surgical specimen reduces accuracy [10].

## 2. Materials and Methods

### 2.1. Collection and Preparation of Patient's Samples

The regulations and rules of the Egyptian National Cancer Institute (NCI) Cairo University governed this study during a period of one year. Ethical approval—including patient consent—for this study was not necessary, due to the patient samples and their data being taken from the routine clinical investigations from the departments of clinical pathology and diagnostic radiology as anonymous samples. After that, their clinical data results and residual samples were collected anonymously to protect the patients' rights.

Blood samples were collected from 50 samples; ten samples were healthy individuals (5 males and 5 females), 10 samples were diagnosed as high-risk group patients (seven males and three females), and 30 were diagnosed as NSCLC patients (25 males and five females). The NCI clinicians diagnosed NSCLC patients according to the National comprehensive Cancer Network (NCCN) version 5, 2017 [1], routinely clinical investigations, tumor marker and diagnostic radiology were performed, and the results were collected to compare with the LAXS technique. Internationally, the NSCLC distribution according to sex is different from Egypt, where the female is not predominant, which is due to the high-risk group mainly in men (smokers). The distribution of the age of the collected samples for the three groups was lightly matched. There were no patients suffering from NSCLC below 40 years of age, and it started to increase for samples of patients above 40 years up to 69 years of age. The whole clinical data for each group is illustrated in Table 1.

**Table 1.** Clinical data of investigated groups.

	Control	High Risk Group (Smokers)	NSCLC Group
	(n = 10)	(n = 10)	(n = 30)
Mean age (years)	42 ± 3.5	48 ± 3.1	50 ± 9
Sex:			
M	5	7	25
F	5	3	5
UICC stage:			
I	----	----	8
II	----	----	17
III	----	----	5

The thirty NSCLC patients were classified according to their tumor grading; 8 patients (grade I), 17 patients (grade II), and 5 patients (grade III), whereas no grade IV NSCLC patients were included in this study. The patients samples in this study were collected via venipuncture process and were clotted in 37 °C temperature for half hour. Following this, the blood samples were centrifuged for ten minutes at  $5040 \times g$  (3000 rpm). Then, the supernatant patients' sera were separately collected and kept at −80 °C. According to previous research, which was elucidated, the suitable temperature for storing biological samples for long periods was −80 °C, and this condition did not affect the characteristic scattering behavior [7]. The collected samples were lyophilized by using a freeze dryer (Edwards, UK) at minus fifty Celsius and negative vacuum pressure of 6.4 mbar in magnitude for six hours to complete water removal from the samples and then were kept in dry sealed plastic tubes at minus eighty Celsius. For LAXS measurements, the samples had to warm up at room temperature.

## 2.2. Measurements of X-ray Scattering

The lyophilized powdered serum was smeared on glass mounted vertically in the rotating holder of the Shimadzu X-ray diffractometer to investigate the scattering profile for each individual. The operating condition of this instrument was working in reflection geometry at 40 kV and 30 mA, using a copper target to produce the mainly high collimated 8.047 keV X-ray beam. The scattering angles were investigated in this study from 2° up to 30°, with steps of 0.25°. The rotation was in ( $\theta$ – $2\theta$ ) mode. Sodium iodide crystal with a graphite monochromator in a scintillation detector collected the scattering data and interfaced to the computer.

## 2.3. Calculation and Analysis of the Parameters from LAXS Data Profile

Table 2 presents the characterized parameters that were calculated from the LAXS profiles of the patients' sera. Figure 1 elucidated the calculation processes of these parameters. The first parameter was the full width at half maximum for the first and second peaks, which were acronymically known as FWHM<sub>1</sub> and FWHM<sub>2</sub>, which had the scattering degrees 4.8° and 10.5°, respectively.

To estimate FWHM, the base line for each peak was plotted, which made references to calculate their values, as illustrated in Figure 1. The percentage ratio of the first and second scattering peaks values ( $I_1/I_2\%$ ) were inserted in Table 2. Moreover, the amplitudes of the rising and falling edges of peaks 1 and 2 were tabulated to represent their values as A<sub>1</sub> and A<sub>2</sub>, respectively.

The final manipulated procedure for the characterized measured parameters was statistically analyzed by using the Statistical Package for the Social Sciences (SPSS) version 24. The representing forms of our data were tabulated as mean ± standard error of the different parameters (Table 2). Analysis of variance (ANOVA) test was used to compare the mean values of each characterized parameter. Individual values for each parameter were used to calculate means. When the compared groups were statistically significant, an

additional test was followed by Duncan's multiple range test to test the discrimination of the investigated groups.

**Table 2.** Mean values of the measured parameters for low-angle X-ray scattering scanned data from normal, high-risk group, and NSCLC serum samples.

	Normal Serum	High Risk Group	NSCLC		
	(n = 10)	(n = 10)	(n = 30)	F-Ratio	p-Value
FWHM <sub>1</sub> (deg)	1.96 ± 0.12 <sup>a</sup>	1.95 ± 0.2 <sup>a</sup>	2.19 ± 0.20 <sup>b</sup>	4.906	0.0120
FWHM <sub>2</sub> (deg)	5.23 ± 0.14	5.24 ± 0.22	5.39 ± 0.26	1.898	0.1600 <sup>c</sup>
Peak position 1 (deg)	4.78 ± 0.15 <sup>a</sup>	4.93 ± 0.22 <sup>b</sup>	5.08 ± 0.16 <sup>b</sup>	8.515	0.0005
Peak position 2 (deg)	10.52 ± 0.16 <sup>a,b</sup>	10.45 ± 0.22 <sup>a</sup>	10.62 ± 0.13 <sup>b</sup>	3.878	0.0270
I <sub>1</sub> /I <sub>2</sub> %	55.14 ± 2.32 <sup>a</sup>	54.20 ± 1.42 <sup>a,b</sup>	53.10 ± 1.74 <sup>b</sup>	3.324	0.0440
A <sub>2</sub> /A <sub>1</sub> %	45.64 ± 5.80 <sup>a</sup>	38.20 ± 3.82 <sup>b</sup>	33.80 ± 3.81 <sup>b</sup>	11.411	0.0001
Counts under peak 1	7.12 ± 0.22 <sup>a</sup>	6.99 ± 0.16 <sup>a</sup>	6.62 ± 0.19 <sup>b</sup>	20.112	0.0001

<sup>a</sup> Statistically classified group a. <sup>b</sup> Statistically classified group b which is significantly different to group a. <sup>c</sup> NS: non-significant.

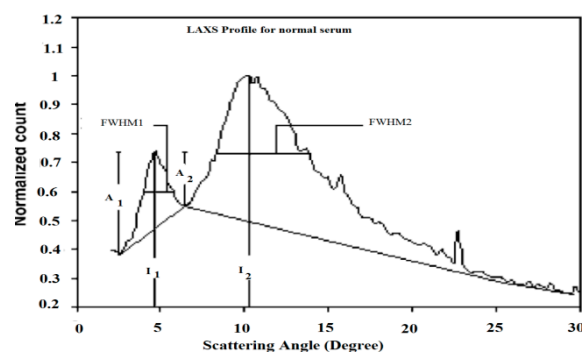


**Figure 1.** The calculation of the characterized parameters measured from the scattering profile of normal serum.

According to the world health organization (WHO) classification, NSCLC is distributed by more than 80% among lung cancer patients [1]; moreover, the latent diagnosis of NSCLS is mainly a medical problem due to the advanced cancer stage. While the routine medical investigation is dependent on general signs and symptoms in addition to laboratory markers, the results from these finds are diagnostically supported by radiologic imaging (PET/CT scan, brain MRI).

### 3. Results and Discussion

The LAXS characterized parameters are shown in Figure 1 for the normal sample. The high-risk group and NSCLC samples are presented in Table 2. To be easily comparable and applicable, all graphs were normalized to unify at the second peak of scattering at 10.5°, and a maximum three-point average was plotted for each graph. Figure 2 elucidates the present of two relatively broad scattering peaks, which were analyzed in this study, whereas a number of sharp diffraction peaks were presented due to the NaCl crystals in serum sample [8]. The sharp peak amplitudes differed from individual samples according to their NaCl concentrations. In an overview of Figure 2, there are clear differences in the first peak at 4.8° for the NSCLC and normal individuals. The calculated parameters are tabulated in Table 2, which contains the full width at the half maximum of peak one (FWHM<sub>1</sub>) for the NSCLC group, which was significantly the highest value compared to the normal and high-risk groups. The difference between the normal and high-risk groups was not significant. Moreover, there was a significant shift in the first scattering peak position from 4.8° for healthy individuals to 4.9° for the high-risk group, up to 5.1° for the NSCLC samples. The shift difference in the high-risk and NSCLC groups was non-significant (Table 2).

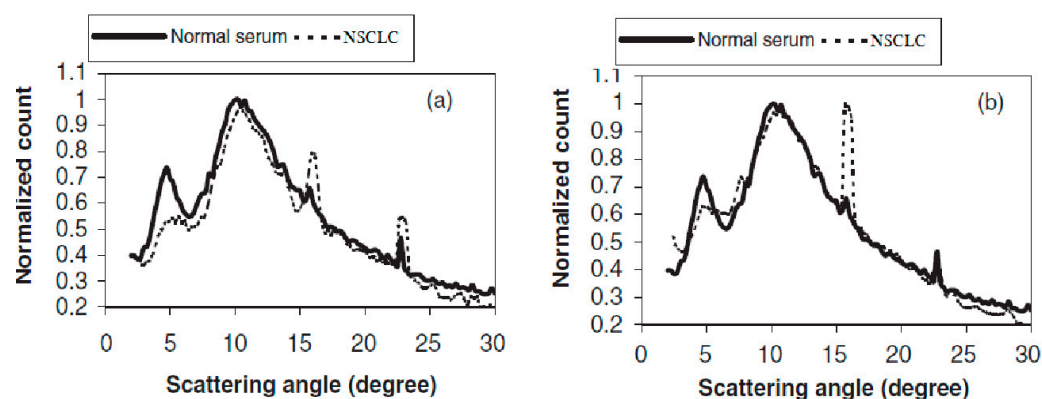


**Figure 2.** LAXS profiles of NSCLC compared to normal individual.

The percentage of the amplitude ratio of the first to second peaks ( $I_1/I_2$  %) found a few decreases in their values in the NSCLC and high-risk groups compared to the healthy group. The only significant difference was between the healthy and high-risk groups. Peak one consisted of a raising edge ( $A_1$ ) and a falling edge ( $A_2$ ), and the resulting dividing ratio ( $A_2/A_1$ ) was mentioned in percentage form in Table 2. This peak had a unique behavior concerned with its amalgamation of the falling edge of the first peak, with the second scattering peak that affected the height  $A_2$  being lower than  $A_1$ .

The percentage ratio of ( $A_2/A_1$ ) represent a significant difference between the normal and NSCLC groups with a high standard error. The high-risk group's percentage ratio of ( $A_2/A_1$ ) was in between the normal and NSCLC groups and had a significant difference compared with the healthy group, represented in Table 2. The shape of the first scattering peak was illustrated in Figure 2; this realized that its shape was different in all NSCLC samples compared to the normal samples.

The first scattering peak was distorted, which was clearly observed in all NSCLC profiles, regardless of the varieties of the peak shape distortion in each individual sample. A decrease in the area under the first peak compared to health group profile was commonly observed in all NSCLC profiles. Moreover, the area under the peak, which is known as counts under peak one, was significantly decreased in the NSCLC group compared to the health group. This parameter is tabulated and represented in Table 2.

The substantial finding in this research was concise and as follows: significant six characterization parameters could be discriminated in two of the three investigated groups.  $FWHM_2$  had a non-significant diversity between all groups (refer to Table 2). The significant differences between the normal and NSCLC groups in the parameters  $FWHM_1$ , peak position 1, ( $I_1/I_2$ %), ( $A_1/A_2$ %), and counts under peak 1 were found. The parameters could have been using a significant discrimination between the healthy and high-risk groups with two parameters, peak position one and ( $A_2/A_1$ %), and three parameters elucidated significant differences between the NSCLC and high-risk groups,  $FWHM_1$ , peak position two, and counts under peak one. The alterations chiefly found in the characterized parameters in the first peak of scattering in all groups could have been referring to the previous studies that confirmed the sensitivity of this peak toward the alterations of the protein structure [10,11]. It was previously published that the scattering profile of irradiated serum had a distortion in its first scattering peak. Evidently, there was no statistical correlation among the observed differences in the characterized parameters as a result of the age of the three groups of individuals.

The LAXS technique beats the main clinical problem that arises in the diagnosis and treatment of NSCLC, which results from lung tissue motions during breaths that cause a variations in density; hence, it gives inaccurate data, especially in early stage (tumor location and size) [11]. To solve this clinical problem, the four dimensions computed tomography (4DCT) technique is used to capturing respiratory motion, creating an individual dynamic data for each patient. The correlation between the analyzed 4DCT images in an



NSCLC patient and their tumor size is significantly proved in its location and classified clinical stage [6,12]. In contrast to the sophisticated procedures and analysis of the 4DCT, the LAXS technique is predominant in simplicity, featuring no radiation hazard for the patient. Moreover, it has a high level of accuracy, which is independent on the tumor location and size.

#### 4. Conclusions

According to the definition from the National Institutes of Health, LAXS could be used as a good biomarker due to its objectively measurable characterization, its ability to evaluate, its unique indicator of normal biologic processes, and its ability to recognize pathogenic processes. Moreover, clinical decision-making could be improved [6]. In addition to all the previously mentioned criteria, the LAXS technique is a cheap, specific, and durable technique, with a great advantage that avoids the radiation hazard through ordinary radiologic investigations for NSCLC patients.

**Author Contributions:** Conceptualization, M.S.M.; methodology, A.M.S.M. and M.S.M.; software, A.M.S.M. and M.S.M.; validation, M.S.M. and A.M.S.M.; formal analysis, M.S.M.; investigation, M.S.M.; resources, M.S.M. and A.M.S.M.; data curation, M.S.M.; writing—original draft preparation, A.M.S.M.; writing—review and editing, M.S.M.; visualization, M.S.M.; supervision, M.S.M.; project administration, M.S.M.; funding acquisition, M.S.M. All authors have read and agreed to the published version of the manuscript.

**Funding:** This research received no external funding.

**Institutional Review Board Statement:** This study doesn't need ethical approval due to the residual sample was anonymously collected after its clinical routine investigation.

**Informed Consent Statement:** Patient consent was waived due to the residual samples were collected to this study from clinical pathology laboratory, after the routine clinical investigations (tumor markers), were done, then, the residual samples were collected to this study.

**Data Availability Statement:** Not applicable.

**Conflicts of Interest:** The authors declare no conflict of interest.

#### References

1. Ettinger, D.S.; Wood, D.E.; Aisner, D.L.; Akerley, W.; Bauman, J.; Chirieac, L.R.; D'Amico, T.A.; DeCamp, M.M.; Dilling, T.J.; Dobelbower, M.; et al. Non-Small Cell Lung Cancer, Version 5.2017, NCCN Clinical Practice Guidelines in Oncology. *J. Natl. Compr. Canc. Netw.* **2017**, *15*, 504–535. [[CrossRef](#)] [[PubMed](#)]
2. Silvestri, G.A.; Gould, M.K.; Margolis, M.L.; Tanoue, L.T.; McCrory, D.; Toloza, E.; Detterbeck, F. Noninvasive staging of non-small cell lung cancer: ACCP evidenced-based clinical practice guidelines (2nd edition). *Chest* **2007**, *132*, 178S–201S. [[CrossRef](#)]
3. De Wever, W.; Vankan, Y.; Stroobants, S.; Verschakelen, J. Detection of extrapulmonary lesions with integrated PET/CT in the staging of lung cancer. *Eur. Respir. J.* **2007**, *29*, 995–1002. [[CrossRef](#)]
4. Zamay, T.N.; Zamay, G.S.; Kolovskaya, O.S.; Zukov, R.A.; Petrova, M.M.; Gargaun, A.; Berezovski, M.V.; Kichkailo, A.S. Current and prospective protein biomarkers of lung cancer. *Cancers* **2017**, *9*, 155. [[CrossRef](#)]
5. Liu, L.; Teng, J.; Zhang, L.; Cong, P.; Yao, Y.; Sun, G.; Liu, Z.; Yu, T.; Liu, M. The Combination of the Tumor Markers Suggests the Histological Diagnosis of Lung Cancer. *Biomed Res. Int.* **2017**, *2017*, 2013989. [[CrossRef](#)] [[PubMed](#)]
6. Seijo, L.M.; Peled, N.; Ajona, D.; Boeri, M.; Field, J.K.; Sozzi, G.; Pio, R.; Zulueta, J.J.; Spira, A.; Massion, P.P.; et al. Biomarkers in Lung Cancer Screening: Achievements, Promises, and Challenges. *J. Thorac. Oncol.* **2019**, *14*, 343–357. [[CrossRef](#)] [[PubMed](#)]
7. Elshemey, W.M.; Desouky, O.S.; Mohammed, M.S.; Elsayed, A.A.; el-Houseini, M.E. Characterization of cirrhosis and hepatocellular carcinoma using low-angle X-ray scattering signatures of serum. *Phys. Med. Biol.* **2003**, *48*, N239–N246. [[CrossRef](#)] [[PubMed](#)]
8. Desouky, O.S.; Elshemey, W.M.; Selim, N.S.; Ashour, A.H. Analysis of low-angle X-ray scattering peaks from lyophilized biological samples. *Phys. Med. Biol.* **2001**, *46*, 2099–2106. [[CrossRef](#)] [[PubMed](#)]
9. Elshemey, W.M.; Desouky, O.S.; Ashour, A.H. Low-angle X-ray scattering from lyophilized blood constituents. *Phys. Med. Biol.* **2001**, *46*, 531–539. [[CrossRef](#)] [[PubMed](#)]
10. Howlader, N.; Noone, A.M.; Krapcho, M.; Miller, D.; Bishop, K.; Altekruse, S.F.; Kosary, C.L.; Yu, M.; Ruhl, J.; Tatalovich, Z.; et al. *SEER Cancer Statistics Review, 1975–2013, Based on November 2015 SEER Data Submission, Posted to the SEER Web Site, April 2016*; National Cancer Institute: Bethesda, MD, USA, 2016.

11. Li, H.; Dong, L.; Bert, C.; Chang, J.; Flampouri, S.; Jee, K.W.; Lin, L.; Moyers, M.; Mori, S.; Rottmann, J.; et al. AAPM Task Group Report 290: Respiratory motion management for particle therapy. *Med. Phys.* **2022**, *49*, e50–e81. [[CrossRef](#)] [[PubMed](#)]
12. Chen, Z.; Huang, L.; Zhu, B. Assessment of Seven Clinical Tumor Markers in Diagnosis of Non-Small-Cell Lung Cancer. *Dis. Markers* **2018**, *2018*, 9845123. [[CrossRef](#)] [[PubMed](#)]

**Disclaimer/Publisher's Note:** The statements, opinions and data contained in all publications are solely those of the individual author(s) and contributor(s) and not of MDPI and/or the editor(s). MDPI and/or the editor(s) disclaim responsibility for any injury to people or property resulting from any ideas, methods, instructions or products referred to in the content.